Vertical split-ring resonator based nanoplasmonic sensor

Pin Chieh Wu,[1] Greg Sun,[2] Wei Ting Chen,[1] Kuang-Yu Yang,[3] Yao-Wei Huang,[1] Yi-Hao Chen,[1] Hsiang Lin Huang,[4] Wei-Lun Hsu,[1] Hai Pang Chiang,[3,4,5,a)] and Din Ping Tsai[1,3,a)]

[1]*Department of Physics, National Taiwan University, Taipei 10617, Taiwan*
[2]*Department of Engineering, University of Massachusetts Boston, Boston, Massachusetts 02125, USA*
[3]*Research Center for Applied Sciences, Academia Sinica, Taipei 11529, Taiwan*
[4]*Institute of Optoelectronic Sciences, National Taiwan Ocean University, Keelung 20224, Taiwan*
[5]*Institute of Physics, Academia Sinica, Taipei 11529, Taiwan*

(Received 16 June 2014; accepted 14 July 2014; published online 21 July 2014)

Split-ring resonators (SRRs) have been the subject of investigation as plasmonic sensors that operate by sensing plasmon resonance shift $\delta\lambda$ when exposed to a medium with a refractive index change δn. However, conventional planar SRRs have their plasmon fields spread into the substrates, reducing accessible sensing volume and its sensing performance. Such a limitation can be eradicated with vertical SRRs in which the plasmon fields localized in SRR gaps are lifted off from the substrate, allowing for greatly enhanced sensitivity. Here, we demonstrate the highest sensitivity among reported SRR-based sensors in optical frequencies. [http://dx.doi.org/10.1063/1.4891234]

Plasmonic metamaterials are artificially constructed media with extraordinary properties that are derived from periodical sub-wavelength constituent elements typically involving metal with hosting dielectric.[1] These properties of the metamaterials are often times intrinsically connected to the localized surface plasmon (SP) resonances (LSPR) arising from the collective oscillations of free electrons which induce strong electromagnetic fields adjacent to the artificial sub-wavelength metallic elements in the metamaterials.[2–4] The resonance wavelengths are determined by feature geometries of metamaterial elements and their surrounding environment, and thus can be tuned by either changing the element dimensions or the surrounding dielectric.[5–7] Such a property can be explored for a variety of applications,[8–13] one of which is sensing based on the following general design principle. Depending on the wavelength range of interest, a metamaterial consisting of subwavelength metal elements of specific shape and sizes is fabricated on a given substrate. These metal elements exhibit different resonance shifts when exposed to media of different indexes of refraction, and by optically probing the shift, the media to which the metamaterial is exposed is then identified.[14] The motivation of exploring metamaterials for the sensing application is the potential for achieving high sensitivity.[15–18] To this end, metamaterials require to possess strong plasmon resonance features that are sensitive to environment change.[19,20] The split-ring resonator (SRR) is such a metal structure that is typically used as a building block for metamaterials because of its strong resonance accompanied with strong field enhancement within the SRR gap.[21–23] One important measure of a metamaterial sensor is its sensitivity characterized as the ratio of LSPR shift to the change in refractive index of its nearby sensing medium ($\delta\lambda/\delta$n), or spectral shift per refractive index unit (RIU).[24] Obviously, in order to obtain high sensitivity, it is important to have significant portion of the localized fields associated with the plasmon excitation exposed to the sensing medium for a greater resonance shift.[19] Unfortunately, a majority of the metamaterials reported so far have planar SRRs that lie flat on substrates, resulting in a rather appreciable fraction of the plasmon energy distributed in the dielectric substrate below as shown in Fig. 1 which limits the effective sensing volume as well as the sensing performance. This reality is the direct consequence of significant technical challenges in the fabrication because metamaterials are far more easily constructed with planar sub-wavelength elements on substrates. Although a couple of published works show that the sensing volume can be increased by raising up the plasmonic elements on dielectric pillars, a fraction of the localized fields still leaks into the dielectric material underneath.[19,25,26] In this work, we report the fabrication of vertical SRRs (VSRRs) capable of lifting essentially all of the localized fields above the supporting substrate they stand on as illustrated in Fig. 2(a). It has been theoretically predicted that the sensitivity

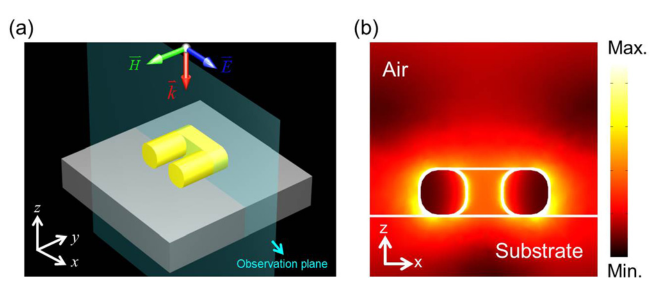

FIG. 1. (a) Schematic diagram of gold planar SRR structure sitting on the top of a fused silica substrate. (b) Electric field distribution in a gold planar SRR under plasmon excitation. The observation screen is marked as a transparent plane in (a). A significant field penetrates into the substrate in the planar SRR configuration, causing a reduced sensing volume.

a)Authors to whom correspondence should be addressed. Electronic addresses: hpchiang@mail.ntou.edu.tw and dptsai@phys.ntu.edu.tw

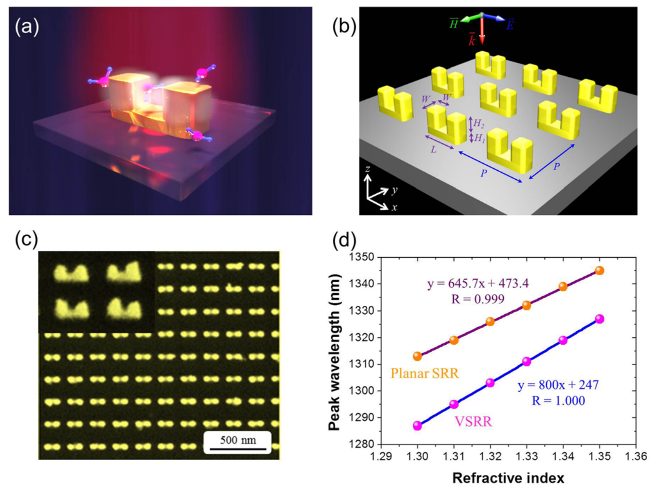

FIG. 2. (a) Illustration of the field distribution in the VSRR gap and its advantage for increasing sensing volume. (b) Schematic diagram for the VSRR array with feature sizes: length of base rod $L = 110$ nm, thickness of base rod $H_1 = 20$ nm, prong length of VSRR structure $H_2 = 60$ nm, prong width $W = 40$ nm, and period $P = 200$ nm. (c) The top and 45° oblique enlarged (inset) SEM images of the fabricated structure. (d) Comparison of sensitivity between VSRRs and planar SRRs of equal dimensions sitting on the same fused silica substrate.

approaching 1400 nm/RIU can be achieved with VSRRs.[27] Using Fourier transform infrared spectroscopy (FTIR) measurement and numerical simulation software (COMSOL Multiphysics), we demonstrate that plasmonic refractive index sensors constructed of VSRRs deliver significantly improved sensitivity over their planar counterparts reported in the literature.

Figure 2(a) shows the schematic concept of our designed VSRR structure standing up vertically on a fused silica substrate under normal illumination. This upright configuration strongly confines the electromagnetic field within the gap as the magnetic plasmon is excited, suspending the enhanced field entirely in the free space away from the dielectric substrate and thus increasing the sensing volume. Electron-beam lithography combined with our recently developed alignment technique is used to fabricate the plasmonic metamaterial composed of VSRRs. The fabrication involves the following steps, (1) Two cross alignment marks with 100 nm thickness are deposited by electron-beam lithography on a fused silica substrate; (2) a layer of 495k PMMA (polymethyl methacrylate) of 180 nm thick is spin-coated and then baked at 180 °C for 3 min; (3) the conductive polymer Espacer (Kokusai Eisei Co., Showa Denso Group, Japan) is spin-coated over the PMMA to eliminate the charging problem during the electron-beam exposure process; (4) an electron-beam system (Elionix ELS-7000) at the acceleration voltage of 100 keV with 30 pA current is used for defining the patterns; (5) the sample was rinsed with de-ionized water to remove Espacer and then developed in solution of methyl isobutyl ketone (MIBK) and isopropyl alcohol (IPA) of MIBK: IPA = 1:3 for 60 s; (6) after the development, a gold thin film was deposited on the sample by thermal evaporation and then the base rod of VSRR structure was defined after the lift-off process; (7) the two prongs of VSRR are fabricated by a second e-beam exposure and lift-off process. Figure 2(b) shows the schematic diagram of the VSRR array standing upright on a substrate with their structural dimensions given in the caption. In order to excite the magnetic plasmon resonance, we use normal incident wave with its electric field (in x direction) polarized in parallel to the SRR base rod and the magnetic field (in y direction) perpendicular to the SRR plane (in y direction). Under this excitation condition, both the incident electric and magnetic fields provide the required component for creating magnetic dipolar response of the VSRRs that generates strongly localized fields within the SRR gaps.[28] Figure 2(c) shows the top and 45° oblique (inset) views of SEM images of the fabricated sample. The enlarged SEM image clearly shows that the two prongs that form the vertical arms of a SRR sit precisely on the two ends of the SRR base rod. Our comparison of sensitivity using simulation as described below has revealed that while $\delta\lambda/\delta n = 645.7$ nm/RIU can be obtained for planar SRRs that lie flat on the fused silica substrate, the slope can be increased to about 800 nm/RIU for the same SRRs but standing up vertically (Fig. 2(d)).

The transmittance spectra of the VSRRs obtained by measurement and simulation are shown in Fig. 3(a) where a pronounced plasmon resonance at $\lambda \sim 1050$ nm is present. Simulation results are obtained by solving three-dimensional Maxwell equation with COMSOL Multiphysics software package. The refractive index of fused silica substrate is fixed at 1.4584. The permittivity of gold in the optical regime is described by the Drude-Lorentz model with plasmon frequency $\omega_p = 8.997$ eV and damping constant $\Gamma_p = 0.14$ eV. Because of the surface defect scattering and grain effects of real samples, the damping constant we used is two times larger than the bulk value. Transmittance spectra are measured using Bruker VERTEX 70 Fourier-transform infrared spectrometer with Bruker HYPERION 1000 infrared microscope (15× Cassegrain objective, numerical aperture NA = 0.4, near-infrared polarizer, and an InGaAs detector). An iris is used to collect the incident light to a square area of about $75 \times 75\ \mu m^2$. The small resonance shift and broader resonance dip observed in the measurement reflect the result of VSRR size variation and roughness of the fabricated sample that deviate from the exact dimensions and boundary condition of perfectly smooth structures used in the simulation. The desirable situation for achieving high sensitivity by exposing more SRR sensing volume to air is clearly illustrated in Fig. 3(b) by the simulation of electric field intensity distribution around the VSRR. From the side and top views of the intensity distribution in Fig. 3(b), it can be seen that the electric field associated the magnetic plasmon excitation is largely localized within the VSRR gap closer to the top of the structure, raising the sensing volume away from its substrate where the medium to be detected can easily displace the air to cause a refractive index change surrounding the VSRR and thus causing a resonance shift to be recorded. To present a complete picture, Figs. 3(c) and 3(d) show the side and top views of the magnetic field intensity and Poynting vector around the VSRR, respectively. Both confirm the fact that the electromagnetic energy and flow are strongly confined within the VSRR gap away from the dielectric substrate.

To demonstrate and examine the sensing performance of the VSRR structure, we have performed the sensitivity

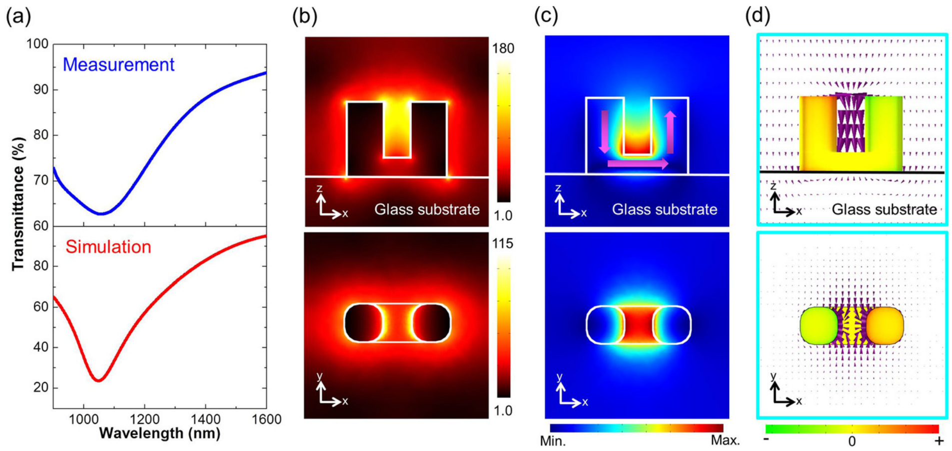

FIG. 3. (a) Experimental and simulation transmittance spectra of the VSRRs sitting on a silica substrate exposed to air. (b) Intensity of electric field in arbitrary unit for the side and top views at the plasmon resonance. (c) Magnetic field intensity distribution of the side and top views at resonance with the arrows pointing in the direction of induced current at a particular moment. (d) Surface charge distribution of the side and top views at resonance. The purple arrows represent the Poynting vector. All side views of the simulation results are obtained at the *x-z* plane in the middle of VSRR, all the top views are in the *x-y* plane ($z = 20$ nm) right on top of the SRR base rod.

analysis by experiment and simulation. Figure 4(a) shows the transmittance spectra when the VSRRs are emerged in liquids of two different refractive indexes. All the refractive index matching liquids used here are the commercial products purchased from Cargille Labs. As the refractive index of the SRR environment is changed from air to 1.32 and 1.33, the resonance dip of measured spectrum is shifted from 1058 nm to 1236 nm and 1254 nm, respectively. The simulation result is in good agreement with the measurement, showing resonance shift to longer wavelength with the increase of surrounding refractive index as shown in Fig. 4(a). In order to see clearly the spectral shift of magnetic resonance with the various refractive index liquid, a zoom-in simulation transmittance spectrum is performed (Fig. 4(c)). Using a linear fit, the simulation has predicted a sensitivity of about $\delta\lambda/\delta n = 797$ nm/RIU, while our measurement has

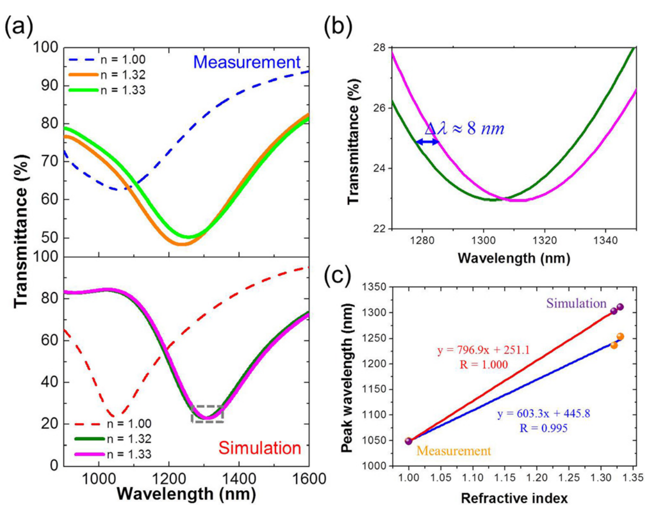

FIG. 4. (a) Experimental and simulation transmittance spectra of the VSRRs immersed in liquids of refractive indexes of $n = 1.32$ and 1.33. The optical spectrum for air ($n = 1.00$) is also plotted (dashed line) for comparison. (b) Enlarged simulation transmittance spectra for magnetic resonance dip in the spectral region indicated with the dashed box in (a). (c) The resonance wavelength associated with the plasmon resonance of experimental (orange dots) and simulation (purple dots) results as a function of the surrounding refractive index.

produced a less value of 603 nm/RIU. It is interesting to point out that our transmittance measurement has yielded spectral resonance shift between the two different liquids greater than what was predicted by the simulation.

The sensitivity produced from the simple isolated VSRR sample, that is, by no means optimized is better or on par with those obtained from planar SRR structures that are more complex and require more elaborate design. Combining a planar SRR structure with a nanodisk, Zhang *et al.* have demonstrated that the coupling between sharp high-order magnetic mode and broad electric dipole mode gives a sensitivity of about 282 nm/RIU.[29] The sensitivity of planar SRR based plasmonic sensor has been further improved to 636 nm/RIU under appropriate design and arrangement of a unit cell that contains four rotationally symmetric SRRs.[21] By using a cylindrical SRR-like cross section structure, sensitivity of nearly 600 nm/RIU has been demonstrated due to the larger sensing cross section and field enhancement.[30] While higher sensitivities around 1000 nm/RIU in other non-SRR plasmonic structures with a dielectric lift have been reported,[25,26] the result presented here is the highest sensitivity among SRR-based plasmonic sensors in the optical region to date and we believe further improvement can be obtained by optimizing the VSRRs.

Our recently developed alignment technique has allowed us to fabricate VSRR structures capable of lifting localized plasmon fields off of the substrates. Such a feature is desirable for developing refractive index sensors based on plasmonic structures that respond to environment change with LSPR shift. By reducing the fraction of the plasmon field diffused into substrates, we effectively increase the sensing volume and therefore the sensitivity. We have experimentally demonstrated the sensitivity of 603.3 nm/RIU, while our simulation predicts about 800 nm/RIU from this simple VSRR based sensor. Further improvement is achievable with optimized VSRRs or coupled structures. The employment of VSRR structures in refractive index sensors for biosensing applications is a promising method for achieving ultrahigh sensitivity and label-free properties at low cost.

The authors acknowledge financial support from Ministry of Science and Technology, Taiwan (Grant Nos. 103-2745-M-002-004-ASP, 102-2745-M-002-005-ASP, 102-2911-I-002-505, 100-2112-M-019-003-MY3, and 100-2923-M-002-007-MY3) and Academia Sinica (Grant No. AS-103-TP-A06). They are also grateful to National Center for Theoretical Sciences, Taipei Office, Molecular Imaging Center of National Taiwan University, National Center for High-Performance Computing, Taiwan, and Research Center for Applied Sciences, Academia Sinica, Taiwan for their support. G. Sun acknowledges support from the Air Force Office of Scientific Research (Grant No. FA9550-14-1-0196, Dr. Gernot Pomrenke, Program Manager).

[1] Y. Liu and X. Zhang, Chem. Soc. Rev. **40**(5), 2494–2507 (2011).
[2] A. Kinkhabwala, Z. Yu, S. Fan, Y. Avlasevich, K. Mullen, and W. E. Moerner, Nat. Photonics **3**(11), 654–657 (2009).
[3] P. Nordlander, ACS Nano **3**(3), 488–492 (2009).
[4] J. Ye, F. Wen, H. Sobhani, J. B. Lassiter, P. V. Dorpe, P. Nordlander, and N. J. Halas, Nano Lett. **12**(3), 1660–1667 (2012).
[5] N. Liu, M. Hentschel, T. Weiss, A. P. Alivisatos, and H. Giessen, Science **332**(6036), 1407–1410 (2011).
[6] J. N. Anker, W. P. Hall, O. Lyandres, N. C. Shah, J. Zhao, and R. P. Van Duyne, Nat. Mater. **7**(6), 442–453 (2008).
[7] Z.-G. Dong, H. Liu, J.-X. Cao, T. Li, S.-M. Wang, S.-N. Zhu, and X. Zhang, Appl. Phys. Lett. **97**(11), 114101 (2010).
[8] C. Wu, A. B. Khanikaev, R. Adato, N. Arju, A. A. Yanik, H. Altug, and G. Shvets, Nat. Mater. **11**(1), 69–75 (2012).
[9] J. Ye, M. Shioi, K. Lodewijks, L. Lagae, T. Kawamura, and P. Van Dorpe, Appl. Phys. Lett. **97**(16), 163106 (2010).
[10] C. Cao, J. Zhang, X. Wen, S. L. Dodson, N. T. Dao, L. M. Wong, S. Wang, S. Li, A. T. Phan, and Q. Xiong, ACS Nano **7**(9), 7583–7591 (2013).
[11] N. Liu, S. Mukherjee, K. Bao, Y. Li, L. V. Brown, P. Nordlander, and N. J. Halas, ACS Nano **6**(6), 5482–5488 (2012).
[12] S. Cho, J.-W. Jang, K.-H. Lee, and J. S. Lee, APL Mater. **2**(1), 010703 (2014).
[13] Y. D. Fernandez, L. Sun, T. Gschneidtner, and K. Moth-Poulsen, APL Mater. **2**(1), 010702 (2014).
[14] A. I. Kuznetsov, A. B. Evlyukhin, M. R. Gonçalves, C. Reinhardt, A. Koroleva, M. L. Arnedillo, R. Kiyan, O. Marti, and B. N. Chichkov, ACS Nano **5**(6), 4843–4849 (2011).
[15] H.-P. Chiang, J.-L. Lin, and Z.-W. Chen, Appl. Phys. Lett. **88**(14), 141105 (2006).
[16] T.-C. Peng, W.-C. Lin, C.-W. Chen, D. Tsai, and H.-P. Chiang, Plasmonics **6**(1), 29–34 (2011).
[17] A. V. Kabashin, P. Evans, S. Pastkovsky, W. Hendren, G. A. Wurtz, R. Atkinson, R. Pollard, V. A. Podolskiy, and A. V. Zayats, Nat. Mater. **8**(11), 867–871 (2009).
[18] J. Becker, A. Trügler, A. Jakab, U. Hohenester, and C. Sönnichsen, Plasmonics **5**(2), 161–167 (2010).
[19] A. Dmitriev, C. Hägglund, S. Chen, H. Fredriksson, T. Pakizeh, M. Käll, and D. S. Sutherland, Nano Lett. **8**(11), 3893–3898 (2008).
[20] M. Stewart, C. Anderton, L. Thompson, J. Maria, S. Gray, J. Rogers, and R. Nuzzo, Chem. Rev. **108**(2), 494–521 (2008).
[21] L. Y. M. Tobing, L. Tjahjana, D. H. Zhang, Q. Zhang, and Q. Xiong, Sci. Rep. **3**, 2437 (2013).
[22] M. Decker, I. Staude, I. I. Shishkin, K. B. Samusev, P. Parkinson, V. K. A. Sreenivasan, A. Minovich, A. E. Miroshnichenko, A. Zvyagin, C. Jagadish, D. N. Neshev, and Y. S. Kivshar, Nat. Commun. **4**, 2949 (2013).
[23] W. T. Chen, C. J. Chen, P. C. Wu, S. Sun, L. Zhou, G.-Y. Guo, C. T. Hsiao, K.-Y. Yang, N. I. Zheludev, and D. P. Tsai, Opt. Express **19**(13), 12837–12842 (2011).
[24] R. Ameling and H. Giessen, Laser Photonics Rev. **7**(2), 141–169 (2013).
[25] N. Verellen, P. Van Dorpe, C. Huang, K. Lodewijks, G. A. E. Vandenbosch, L. Lagae, and V. V. Moshchalkov, Nano Lett. **11**(2), 391–397 (2011).
[26] Y. Shen, J. Zhou, T. Liu, Y. Tao, R. Jiang, M. Liu, G. Xiao, J. Zhu, Z.-K. Zhou, X. Wang, C. Jin, and J. Wang, Nat. Commun. **4**, 2381 (2013).
[27] C.-Y. Chen, I.-W. Un, N.-H. Tai, and T.-J. Yen, Opt. Express **17**(17), 15372–15380 (2009).
[28] P. C. Wu, W. T. Chen, K.-Y. Yang, C. T. Hsiao, G. Sun, A. Q. Liu, N. I. Zheludev, and D. P. Tsai, Nanophotonics **1**, 131–138 (2012).
[29] Q. Zhang, X. Wen, G. Li, Q. Ruan, J. Wang, and Q. Xiong, ACS Nano **7**(12), 11071–11078 (2013).
[30] B. Päivänranta, H. Merbold, R. Giannini, L. Büchi, S. Gorelick, C. David, J. F. Löffler, T. Feurer, and Y. Ekinci, ACS Nano **5**(8), 6374–6382 (2011).